Science Advances
AAAS

advances.sciencemag.org/cgi/content/full/5/9/eaau7802/DC1

Supplementary Materials for

Mechanical regulation of bone homeostasis through p130Cas-mediated alleviation of NF-κB activity

T. Miyazaki*, Z. Zhao, Y. Ichihara, D. Yoshino, T. Imamura, K. Sawada, S. Hayano, H. Kamioka, S. Mori, H. Hirata, K. Araki, K. Kawauchi, K. Shigemoto, S. Tanaka, L. F. Bonewald, H. Honda, M. Shinohara, M. Nagao, T. Ogata, I. Harada, Y. Sawada*

*Corresponding author. Email: miyazak14@tmig.or.jp (T.M.); ys454-ind@umin.ac.jp (Y.S.)

Published 25 September 2019, *Sci. Adv.* **5**, eaau7802 (2019)
DOI: 10.1126/sciadv.aau7802

This PDF file includes:

Supplementary Materials

Figure S1

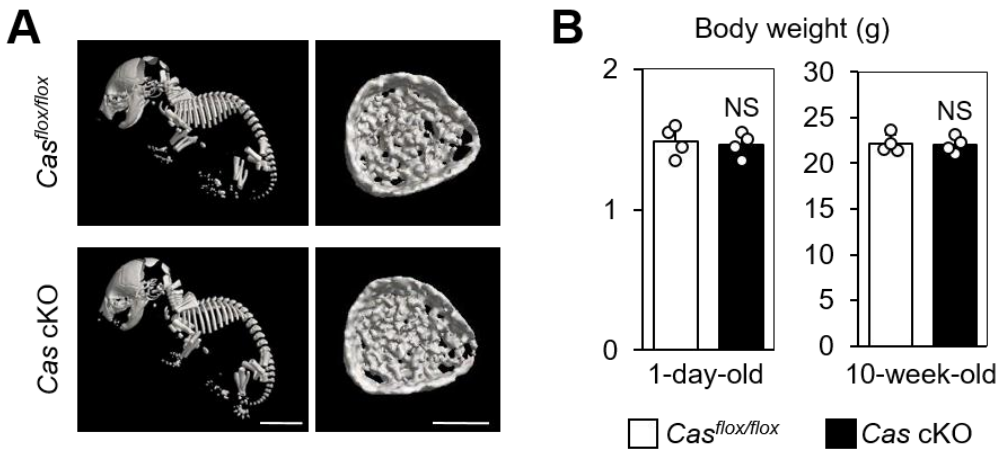

Fig. S1. Skeletal phenotype of *Cas* cKO mice is not distinct at birth. (**A**) μCT analysis of *Cas* cKO newborn mice and their normal *Cas*$^{flox/flox}$ littermates (postnatal day 1, male or female). Left: whole skeleton, right: axial view of metaphyseal femur. Scale bars, 5 mm (left) and 250 μm (right). (**B**) Body weight of *Cas* cKO mice and their normal *Cas*$^{flox/flox}$ littermates at 1 day (male or female) or 10 weeks of age (male) (n = 4 mice per group).

Figure S2

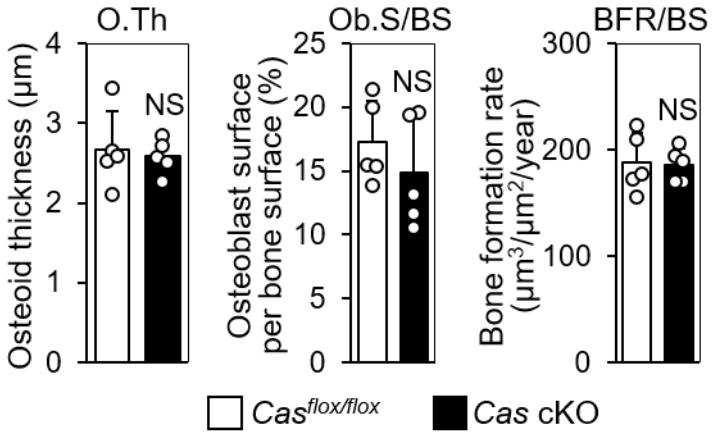

Fig. S2. Bone formation parameters are not significantly altered in *Cas* cKO mice. Parameters for osteoblastic bone formation in *Cas* cKO mice and their normal $Cas^{flox/flox}$ littermates were determined by histomorphometric analysis (n = 5 mice per group).

Figure S3

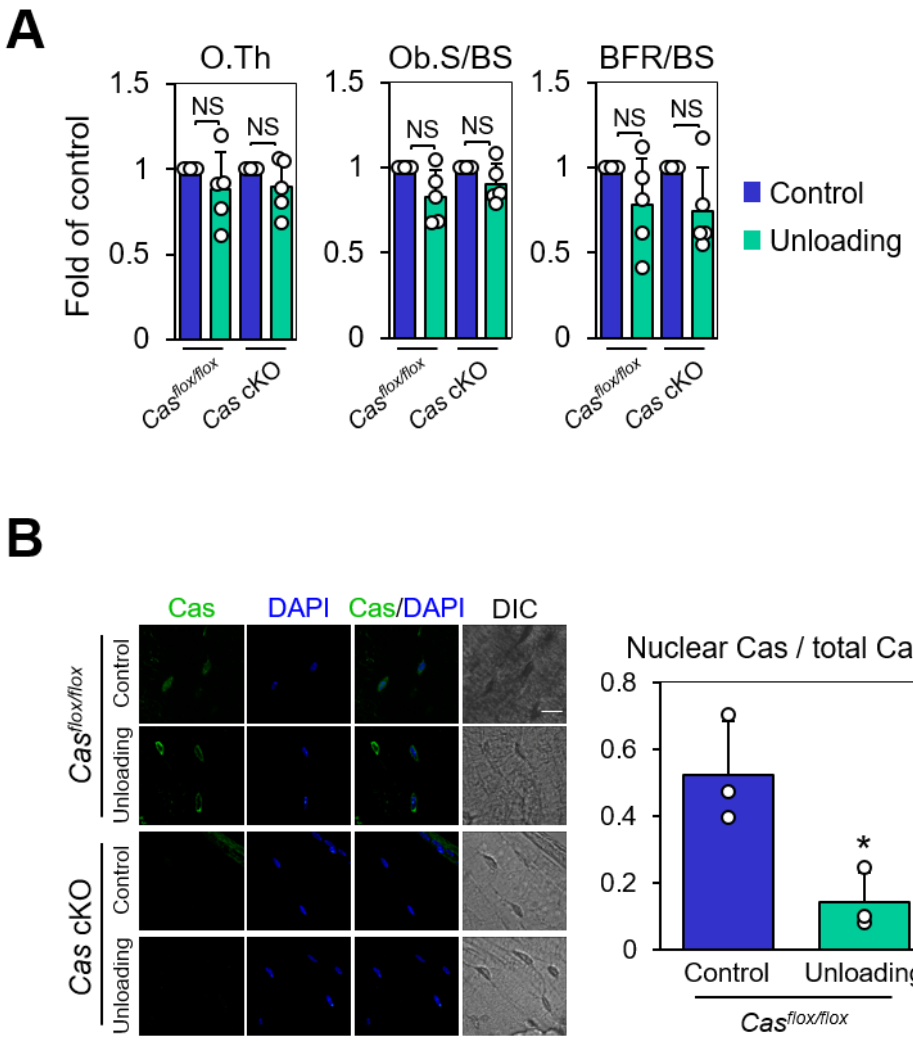

Fig. S3. Mechanical regulation of bone formation in control and *Cas* cKO mice and nuclear distribution of Cas in their osteocytes. (**A**) Bone formation parameters of bones with and without unloading. Values from unloaded bones were normalized against data from their contralateral controls as in Fig. 3B (n = 5 mice per group). (**B**) Mechanical loading-dependent nuclear distribution of Cas in osteocytes. Nuclear distribution of

Cas was analyzed as in Fig. 1B (n = 3 mice per group, each value was averaged from 4 - 6 osteocytes analyzed in each bone).

Figure S4

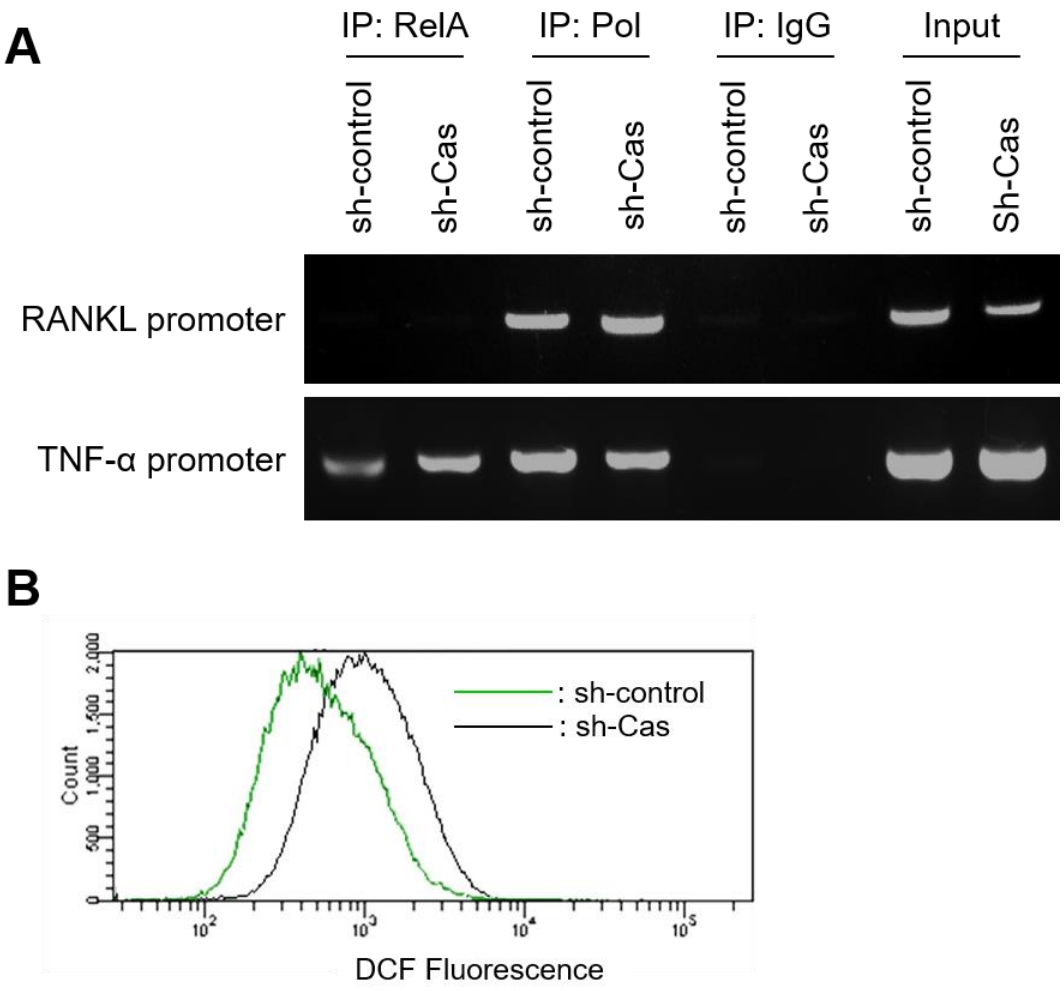

Fig. S4. ChIP analysis of RelA binding to the RANKL promoter region and measurement of intracellular ROS level. (**A**) Absence of detectable RelA binding to the RANKL promoter region in MLO-Y4 osteocytes. ChIP analysis of MLO-Y4 osteocytes was conducted using anti-RelA, anti-polymerase III (Pol, positive control) or anti-IgG (negative control) antibodies. DNA recovered from immunoprecipitates was amplified by PCR using the primers specific for RANKL and TNF-α promoters. (**B**) Measurement of

intracellular ROS level in MLO-Y4 osteocytes with (sh-Cas) and without (sh-control) Cas knockdown by flow cytometry using 2',7'-dichlorodihydrofluorescein (DCF).

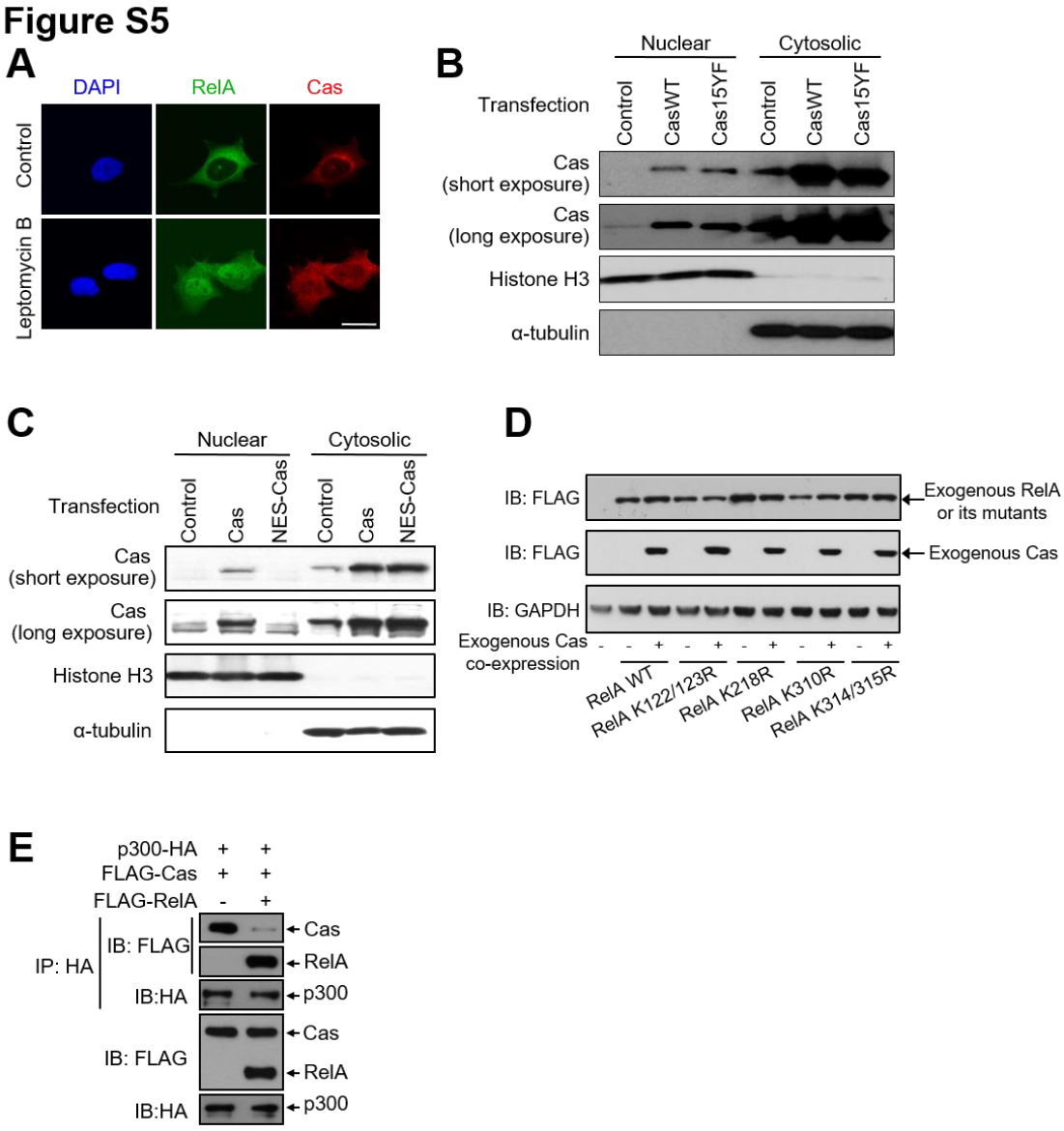

Fig. S5. Cas suppresses RelA acetylation at Lys^{310} in the nucleus and alleviates NF-κB activity without requiring phosphorylation of its substrate domain. (**A**) Cas accumulation in the nucleus after inhibition of nuclear exportation. HEK293 cells, either left untreated or treated with Leptomycin B (10 ng/ml, 6 h), were fixed and subjected to anti-RelA and anti-Cas immunostaining with nuclear staining (DAPI). Scale bar, 10

μm. (**B**) Phosphorylation-independent nuclear distribution of Cas. The nuclear and cytosolic fractions from transfected HEK293 cells were analyzed by immunoblotting. Endogenous Cas was detected in the nuclear fraction by the long exposure of the anti-Cas blot (second row, lane 1). (**C**) Hardly detectable recovery of nuclear export signal (NES)-attached Cas from the nuclear fraction. The nuclear and cytosolic fractions prepared from HEK293 cells transfected with Cas, NES-Cas or their control vector, were analyzed. Endogenous Cas was detected in the nuclear fraction by the long exposure of the anti-Cas blot (second row, lanes 1 and 3). (**D**) The expressions levels of transfected genes in Fig. 5J were evaluated by immunoblotting. (**E**) Attenuation of Cas-p300 interaction by exogenous RelA expression. HEK293 cells, co-transfected with p300-HA and FLAG-Cas together with FLAG-RelA or its control vector, were subjected to co-immunoprecipitation analysis as in Fig. 5K. Note the inverse correlation between RelA and Cas in the immunoprecipitates (see the top and second rows).

Figure S6

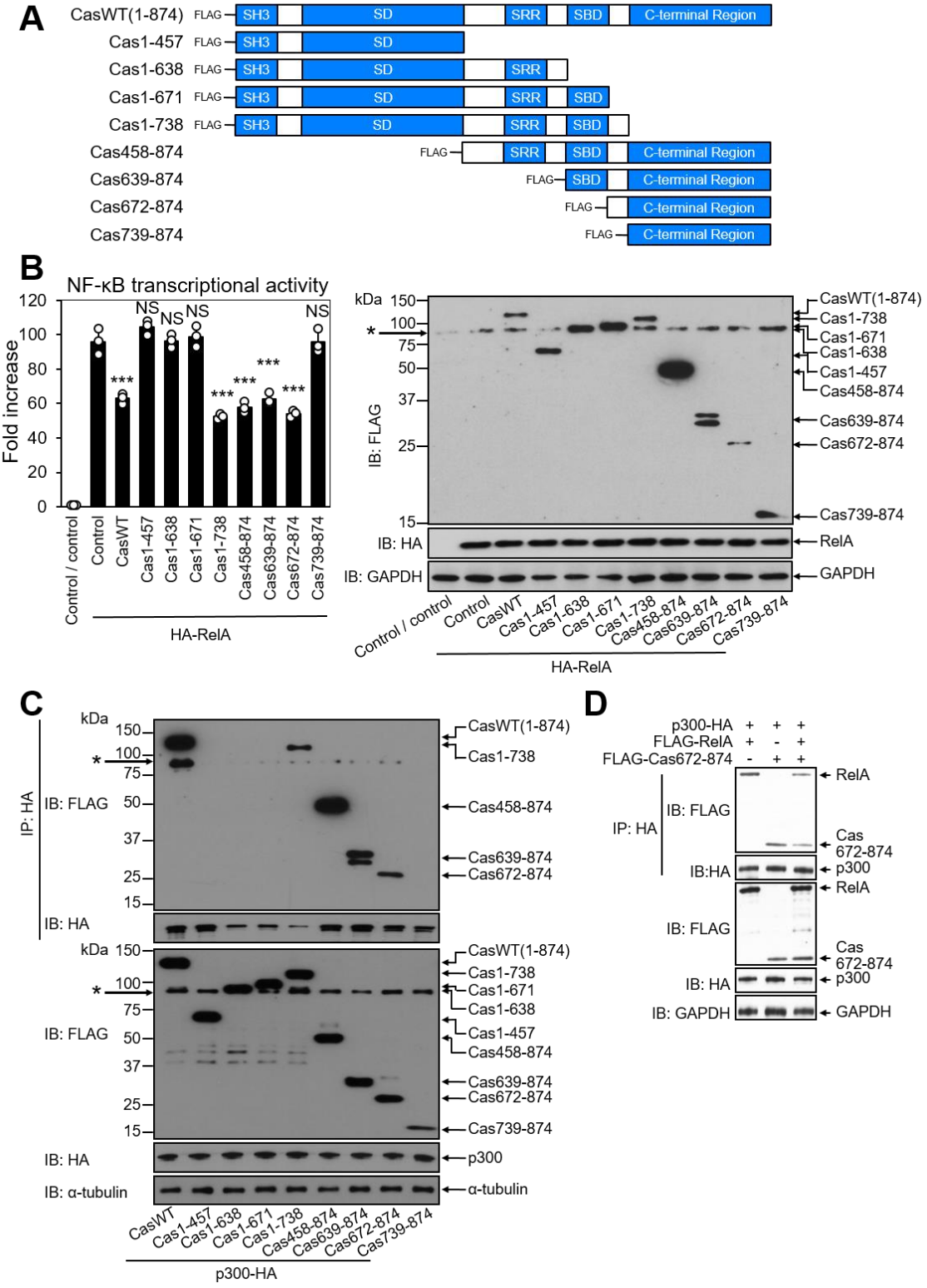
A
CasWT(1-874)
Cas1-457
Cas1-638
Cas1-671
Cas1-738
Cas458-874
Cas639-874
Cas672-874
Cas739-874
FLAG
SH3
SD
SRR
SBD
C-terminal Region
B
NF-κB transcriptional activity
Fold increase
NS
***
Control / control
Control
CasWT
HA-RelA
kDa
IB: FLAG
IB: HA
IB: GAPDH
RelA
GAPDH
C
IP: HA
IB: α-tubulin
p300-HA
p300
α-tubulin
D
p300-HA
FLAG-RelA
FLAG-Cas672-874
IP: HA
IB:HA
Cas 672-874

Fig. S6. Cas672-738 contains the region responsible for the inhibition of NF-κB activity. (**A**) Schematic representation of Cas truncation mutants tested. SH3: Src homology 3; SD: substrate domain; SRR: serine-rich region; SBD: Src-binding domain. (**B**) Suppression of NF-κB transcriptional activity by Cas variants bearing the amino acids 672-738. Luciferase assay was conducted as in Fig. 5C with statistical comparison with the RelA-transfected control sample (column 2) (n = 3) (left). The expression levels of transfected HA-RelA and FLAG-tagged Cas variants were evaluated by immunoblotting. Non-specific binding of the anti-FLAG antibody was observed at ~90 kDa (see an asterisk) (right). (**C**) Co-immunoprecipitation of Cas variants bearing the amino acids 672-738 with p300. HEK293 cells co-transfected with p300-HA and FLAG-tagged Cas variants were subjected to anti-HA immunoprecipitation followed by immunoblot analysis. Non-specific binding of the anti-FLAG antibody was observed as in (B) (see asterisks). (**D**) Inverse correlation between RelA-p300 and Cas672-874-p300 association. Co-expression and co-immunoprecipitation experiments were conducted as in Fig. 5K.

Figure S7

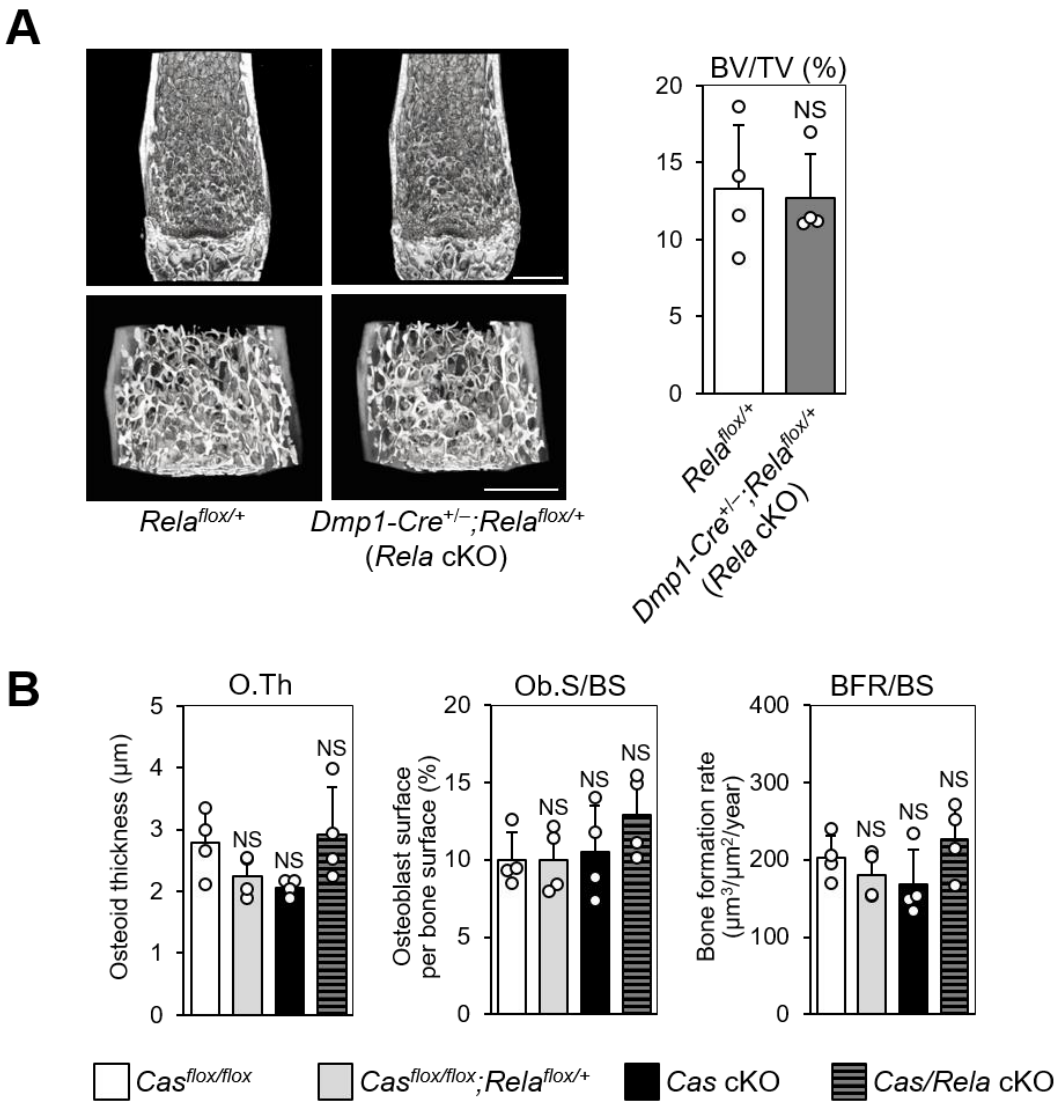

Fig. S7. Neither bone mass of mice with intact *Cas* alleles nor bone formation of *Cas* cKO mice is significantly altered by heterozygous deletion of *Rela* in osteocytes (*Rela* cKO). (**A**) Representative μCT images of distal femurs of *Rela*$^{flox/+}$ (normal control mice) and *Dmp1-Cre*$^{+/-}$*;Rela*$^{flox/+}$ mice (*Rela* cKO mice). Scale bars, 1 mm (left). BV/TV was calculated from μCT images (right, n = 4 mice per group). (**B**)

Histomorphometric parameters for bone formation at tibiae of mice with combinations of *Cas* and *Rela* cKO (n = 4 mice per group, one-way ANOVA with post hoc Bonferroni test).